

CORRELATIONS BETWEEN SLANT WET DELAYS MEASURED BY MICROWAVE RADIOMETRY

Tobias Nilsson, Lubomir Gradinarsky, Gunnar Elgered

*Onsala Space Observatory, Chalmers University of Technology, SE-439 92 Onsala, Sweden,
E-mail address: tobias@oso.chalmers.se (Tobias Nilsson)*

ABSTRACT

We present an analysis of the correlation between the slant wet delays in different directions using data from a microwave radiometer. The correlations between wet delays observed in different directions using different temporal constraints are compared to a model derived from theories of turbulence.

1. INTRODUCTION

The capabilities of using GPS to estimate the total amount of integrated water vapor are well accepted [1]. As the GPS receivers become more accurate and new Global Navigation Satellite Systems (GNSS) are launched providing more satellites in the sky it might be possible to estimate the 3D structure of the refractive index and indirectly also the atmospheric water vapor [2, 3]. In this approach, called GPS tomography, a local network of GPS receivers is utilized. From the data collected by the receivers the slant wet delays the signals experience between the satellites and the receivers can be estimated. By doing a discretization of the atmosphere by dividing it into finite volume pixels (voxels) in which the refractivity is assumed to be constant, an linear system of equations can be solved.

However, in general the system is ill conditioned due to the satellite geometry. This makes it necessary to add additional constraints to make the system solvable. This can be done by using models of the atmospheric turbulence constraining how much the refractivity can vary in space and time [3, 4]. One possibility to obtain information in order to develop or validate such models is to use a water vapor radiometer (WVR) to measure the slant wet delays. In this work the WVR at the Onsala Space Observatory was used to measure the slant wet delays.

2. THEORY

The spatial fluctuations of the wet refractivity in a turbulent atmosphere can be described by a structure function D_χ :

$$D_\chi(\mathbf{r}, \mathbf{R}) = \langle (\chi(\mathbf{r}) - \chi(\mathbf{r} + \mathbf{R}))^2 \rangle = C_n^2 \cdot R^{2/3} \quad (1)$$

where $R = |\mathbf{R}|$ and χ denotes the wet part of the refractivity of the air (equal to refractive index minus one). The constant C_n was estimated to be $C_{n0} = 2.4 \cdot 10^{-7} \text{ m}^{-1/3}$ [5]. This value is based on radiosonde and radiometer

data from California, Australia, and Spain only. It is also likely that C_n has a seasonal dependence because it depends on the amount of water vapor.

The wet delay sensed by WVRs and GPS is the integrated refractivity along the propagation path of the radio signal. The wet delay along ray i (referred to zenith using a mapping function m_i) l_i can be written as:

$$l_i = \frac{1}{m_i} \int \chi(\mathbf{r}_i(z)) ds = \int \chi(\mathbf{r}_i(z)) dz \quad (2)$$

where $\mathbf{r}_i(z)$ is the position of the ray at height z . The correlation between the wet delay in two different directions (i and j) is described by:

$$\langle (l_i - l_j)^2 \rangle = \left\langle \left(\int [\chi(\mathbf{r}_i(z)) - \chi(\mathbf{r}_j(z))] dz \right)^2 \right\rangle \quad (3)$$

In [4] it was shown that this can be rewritten as:

$$\langle (l_i - l_j)^2 \rangle = \sum_{n=1}^{12} a(n) k_n \quad (4)$$

where the coefficients $a(n)$ and k_n are given in [4]. The value of C_n used was that determined in [5] (C_{n0}), and the integrations were performed between the ground and an effective tropospheric height h which was set to $h_0 = 1 \text{ km}$. If the values of these parameters should be different from those it is easily shown that:

$$\begin{aligned} \langle (l_i - l_j)^2 \rangle &= \frac{C_n^2 h^{8/3}}{C_{n0}^2 h_0^{8/3}} \langle (l_i - l_j)^2 \rangle |_{C_n=C_{n0}} \\ &= k \cdot \langle (l_i - l_j)^2 \rangle |_{C_n=C_{n0}} \end{aligned} \quad (5)$$

When measuring the wet delay with a radiometer the effect of the radiometer noise must be considered. Let A denote the radiometer noise expressed in delay. Then the (zenith mapped) wet delay measured by the radiometer, \hat{l}_i in direction i will be:

$$\hat{l}_i = l_i + A \quad (6)$$

It is reasonable to assume that the instrumental noise is independent of Δl , so $\langle \Delta l \Delta A \rangle = \langle \Delta l \rangle \langle \Delta A \rangle$. Since there is no reason why on average the (zenith mapped) wet delay in one direction should be higher than that of another direction, $\langle \Delta l \rangle = 0$. This gives:

$$\langle (\Delta \hat{l})^2 \rangle = \langle (\Delta l)^2 \rangle + \langle (\Delta A)^2 \rangle \quad (7)$$

If the radiometer noise is assumed to be the same in every direction, it will have an elevation dependence when mapped to zenith, so that the measured equivalent zenith wet delays will have a noise term $A(\epsilon) = B/m(\epsilon)$. This gives when inserted into (7):

$$\left\langle (\Delta \hat{l})^2 \right\rangle = k^2 \cdot \left\langle (\Delta l)^2 \right\rangle |_{C_n=C_{n_0}} + (m_i^{-2} + m_j^{-2}) \cdot Var[B] \quad (8)$$

where $\left\langle (\Delta l)^2 \right\rangle |_{C_n=C_{n_0}}$ denotes the value that $\left\langle (\Delta l)^2 \right\rangle$ would have had if C_n and h would be equal to those used in the model.

3. SIMULATIONS

We first assess the model through simulations. Since $\langle l_i - l_j \rangle = 0$, the variance of $l_i - l_j$ will then be $Var[l_i - l_j] = \langle (l_i - l_j)^2 \rangle$, which can be calculated using the model. Assuming that $l_i - l_j$ has a Gaussian distribution, given a set of directions simulated values can be obtained using (4). To simulate the effect of WVR noise, a random number divided by m_i minus another random number divided by m_j was added to each of the simulated values of $l_i - l_j$.

We made simulations using the same set of directions as was used during the acquisitions of the real WVR data. When the simulated values of $(l_i - l_j)^2$ had been obtained a least square fit was made to these values to obtain k^2 and $Var[B]$ in (8). The obtained values could then be compared to those that were used in the simulation.

The simulations show that the values of k^2 and $Var[B]$ can be obtained with a rather good accuracy, the error of the values of k^2 obtained in the simulations was about 5 – 10% for realistic noise levels (standard deviation of a few millimeters) and the noise level was obtained with even better accuracy. However, when the noise was in the order of a few centimeters the estimations became worse. The results of 30 simulations, where $k^2 = 3$ and $Var[B] = 1 \text{ cm}^2$, implied values of k^2 between 1.9 and 3.7, with a mean value of 2.9 and standard deviation 0.4. The noise level was also well determined.

In Fig. 1 the results of the simulations are displayed. Plotted are the simulated values of $\langle (l_i - l_j)^2 \rangle$ including atmospheric variation and instrumental noise together with the model prediction of the atmosphere only and the resulting residual after solving for k^2 and $Var[B]$ as function of the difference in angle. Plotted are the data where one of the directions is in the zenith direction, meaning that the angle difference for the data shown is the difference in elevation. A mean is taken over all observations in 5° intervals to obtain the expectation values.

The top plot in Fig. 1 is for $k^2 = 3$, the variance of the noise being 0.04 cm^2 and the simulation period one full day. As we can see, the residuals are close to zero. However, the simulation is for an ideal case where observations at different times are assumed to

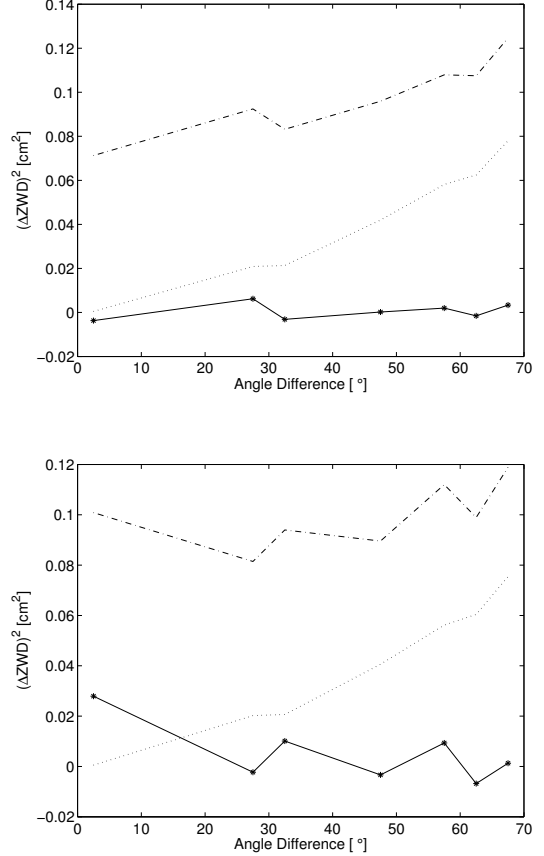


Fig. 1: The result from two simulations. Displayed are the simulated $\langle (l_i - l_j)^2 \rangle$ (dot-dashed line), the model prediction ($k^2 \cdot \langle (l_i - l_j)^2 \rangle |_{C_n=C_{n_0}}$) (dotted line) and the residual ($\langle (l_i - l_j)^2 \rangle - k^2 \cdot \langle (l_i - l_j)^2 \rangle |_{C_n=C_{n_0}} - (m_i^{-2} + m_j^{-2}) \cdot Var[B]$) (solid line with asterisks) as function of the angle difference. The variance of the noise is 0.04 cm^2 in all cases and $k^2 = 3$ for both plots. The simulation periods are one day for the upper and six hours for the lower plot.

be independent. In our case this is not true. This will decrease the information we get from the data, i.e. the same effect as if we would decrease the simulation time. The bottom plot in Fig. 1 is for a simulation time of six hours, $k^2 = 3$ and $Var[B] = 0.04 \text{ cm}^2$. As we see the errors have increased somewhat.

4. EXPERIMENTAL RESULTS

4.1 Maximum time between observations

Since the WVR only can measure in one direction at a time we cannot compare the wet delay in two directions at the same time. The model gives the correlation between the wet delays in two different directions at the same time epoch. So in order to use the WVR data to test the model, the time between the two observations

being compared must be short enough for the change in the wet delays to be negligible.

To assess the impact of the time differences we used WVR data from a whole day and calculated all possible squared differences of (zenith mapped) wet delay for observations being less than Δt_{max} in time from each other. Then a least square fit was made to obtain the values of k^2 and $Var[B]$ in (8) for different values of Δt_{max} and using data from different days in May and June of 2003.

If the change in the wet delay can be neglected the obtained values of k^2 and $Var[B]$ will be independent of the choice of Δt_{max} . The obtained values of k^2 and $Var[B]$ was found to be independent of Δt_{max} for $\Delta t_{max} \lesssim 300$ s. We choose in the following investigations to let Δt_{max} be 300 s, based on this investigation.

4.2 Comparison between model and real data

In Fig. 2 the results from two periods in 2003, 030417–030426 and 030501–030508, are displayed. The chosen data had no liquid water content larger than 0.7 mm. Since the WVR during this time was only making very few measurements in the zenith direction, the data plotted in Fig. 2 is only a small part of the total data, hence the statistics may not be good enough to draw any conclusions from the plots for shorter periods.

The periods in Fig. 2 show very small residuals, hence it can be concluded that the model seem to be correct for these data. However, other periods does not show such a good agreement, but in these some of the disagreement can be explained. In Fig. 3 top the period 030601–030610 is plotted and here the errors are somewhat larger. Some of the errors can possibly be explained by the fact that the values of k^2 seem to have been very large for two of the days. It is likely that data from days with values of k^2 as high as 13.5 might not be very good. A large value of k^2 (and hence C_n) imply large variations in time. Removing these two days from the analysis gives a better agreement with the model as seen in the bottom plot in Fig. 3.

4.3 Seasonal variability of C_n

If we assume that the effective tropospheric height h is approximately constant, a change in k must be due to a change in C_n . Hence, by studying the seasonal variations of k we will see how C_n varies as function of season. In Fig. 4 the values of k obtained from the WVR data from 2000–2002 are plotted as function of season, together with a simple sinusoidal fit made to the data. We see that k (and hence also C_n) reaches its minimum in the middle of February and its maximum the middle of August.

4.4 WVR related issues

In the beginning of 2003 the Onsala WVR was upgraded. In order to detect errors due to instrumental uncertainties a comparison was made between the data taken before and after the upgrade. The mean estimated standard deviations of the noise was 3.3 mm for the investigated data from 2000–2002 and 1.8 mm for the 2003 data.

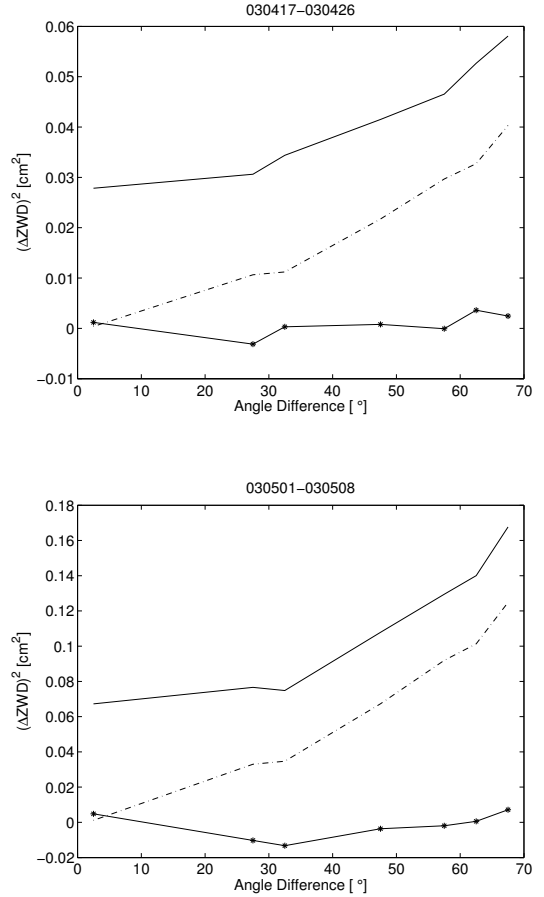


Fig. 2: The result from two periods in 2003. Displayed are the same quantities as in Fig. 1.

Before the upgrade the WVR sometimes produced measurements which were clearly incorrect (they clearly deviated from the rest of the data and were probably caused by a failing analog to digital converter). Such incorrect data could easily be identified and removed if the deviation from the rest of the data is large, but not if the atmosphere shows a large variability. To estimate the effect of this on our results a very crude model for this effect was made. If we remove all data which have a large deviation from nearby observations, the remaining incorrect observations (of the wet delay mapped to zenith) can approximately be described by what would be measured if the radiometer would have worked correctly plus white noise. To account for this we modify (8) by introducing a white noise term W :

$$\left\langle (\Delta l)^2 \right\rangle = k^2 \cdot \left\langle (\Delta l)^2 \right\rangle |_{C_n=C_{n_0}} + (m_i^{-2} + m_j^{-2}) \cdot Var[B] + Var[W] \quad (9)$$

Making a least square fit of the data to (9) to obtain k^2 , $Var[B]$ and $Var[W]$, most of the data taken before the upgrade give a significant positive value of $Var[W]$. Also the deviation between the model and the real data is

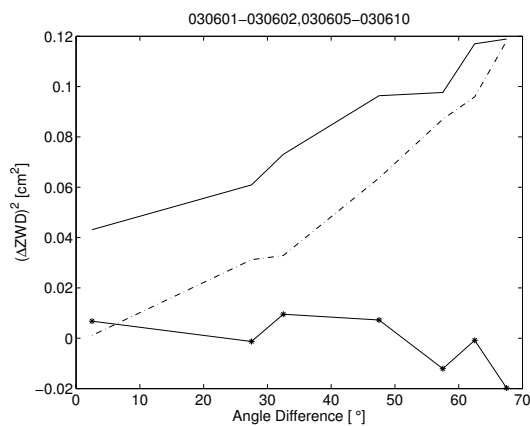
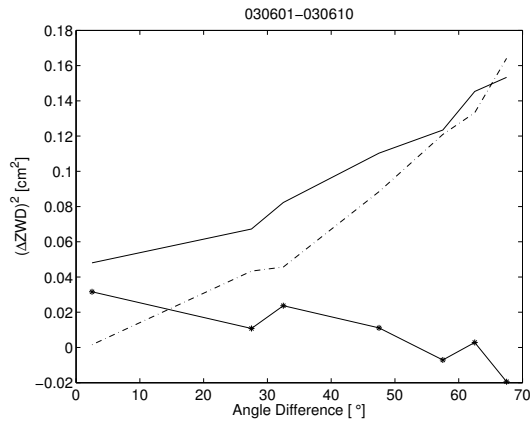


Fig. 3: The result from one periods in 2003, the bottom plot is with the data from two of the days removed (see text). Displayed are the same quantities as in Fig. 1

clearly smaller with the W term included. The retrieved values for $Var[B]$ and k^2 are also somewhat smaller (about 0.03 cm^2 and 0.8) when including the W term. We also observe that that the impact of the incorrect observations tends to be larger in the summer.

If the same analysis is applied on the data taken after the upgrade the obtained values of $Var[W]$ are in most cases small and even negative. The inclusion of the W term does not give any significant reduction of the deviation of the data from the model. From this we may conclude that the number of incorrect observations after the upgrade has been reduced.

5. CONCLUSIONS

Since the agreement between the model and the WVR data seems to be rather good, we can conclude that the model in (1) has been verified. One useful possible application of the model would be to use it as a constraint when estimating slant wet delays from GPS data. Since the equation gives the correlation between the refractivity at two points in space it can be used as

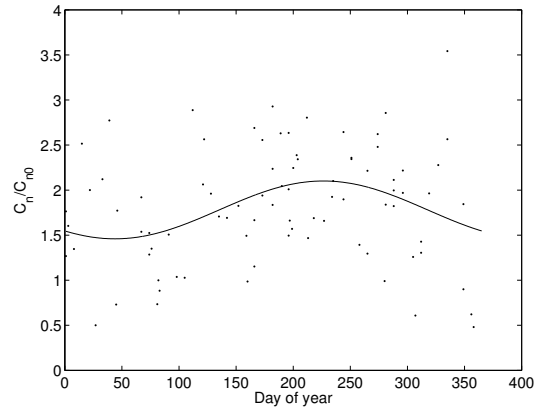


Fig. 4: The seasonal variation of C_n derived from the radiometer data using the model, together with sinusoidal fit.

constraints in GPS tropospheric tomography [3]. Also, using the model in (9) provides information on WVR stability in terms of instrumental noise.

REFERENCES

- [1] L. P. Gradinarsky, J. M. Johansson, H. R. Bouma, H.-G. Scherneck, and G. Elgered, "Climate monitoring using GPS," *Physics and Chemistry of the Earth*, vol. 27, pp. 335–340, 2002.
- [2] A. Flores, J. V.-G. de Arellano, L. P. Gradinarsky, and A. Ruis, "Tomography of the lower troposphere using a small dense network of GPS receivers," *IEEE Trans. Geosci. Remote Sensing*, vol. 39, pp. 439–447, 2001.
- [3] L. Gradinarsky and P. Jarlemark, "Ground-based GPS tomography of water vapor: Analysis of simulated and real data," *J. Meteorol. Soc. Japan*, in press, 2004.
- [4] T. Emardson and P. Jarlemark, "Atmospheric modelling in gps analysis and its effect on the estimated geodetic parameters," *Journal of Geodesy*, vol. 73, pp. 322, 1999.
- [5] R. Treuhaft and G. Lanyi, "The effect of the dynamic wet troposphere on radio interferometric measurements," *Radio Science*, vol. 22, pp. 251–265, 1987.